

# Registration of Short and Long-Axis Images in Cine Cardiac MRI

T. Li<sup>1</sup>, T. S. Denney<sup>1</sup>

<sup>1</sup>Electrical and Computer Engineering, Auburn University, Auburn University, AL, United States

## Introduction

Cardiac MR images acquired over multiple breath-holds are often misregistered due to patient motion or inconsistent respiration. This misregistration must be corrected before three-dimensional (3D) analysis of wall geometry, strain, and other parameters can be performed. Existing registration methods [1, 3] only address the issue of short-axis image registration, but long-axis images are needed to analyze the apex of the heart and can provide information on how the short-axis images should be registered. A new registration method is presented that uses myocardial contours identified in long-axis images to register short-axis images and short-axis contours to register long-axis images. The method is validated on simulated data and imaging studies from 15 human subjects.

## Methods

Fifteen human subjects were imaged with cine cardiac imaging protocol (GE FIESTA). Each study consisted of 11-13 short-axis slices, and a vertical (VLA) and horizontal long-axis (HLA) slice. All slices were 8mm thick with no gap between slices. Endocardial and epicardial contours were identified in each slice at end-diastole and end-systole with a semi-automated algorithm developed in our lab. The short and long-axis slices were then registered to each other at end-diastole and then at end-systole with the following procedure.

First, the short-axis images were registered to each other by fitting a quadratic polynomial to the combined endocardial and epicardial contour centroids. While previously published algorithms [1] used a least-squares fit for this step, this method was too sensitive to large registration errors. Instead, the polynomial coefficients were computed to minimize the absolute value error between the polynomial and centroids. Each short-axis image was then shifted in an in-plane direction so that the centroids in each slice were on the quadratic polynomial line.

Second, the long-axis (VLA and HLA) images were registered to the short-axis contours. In this step, each long-axis slice was translated in 3D to minimize a cost function consisting of two equally-weighted terms. The first term was the average distance from the endocardial and epicardial contours in the long-axis image to the corresponding contour in each short-axis slice. The second term, called the apex distance term, was the distance from the long-axis contour to the most apical short-axis slice. This last term penalizes solutions where the apex in a long-axis slice is closer to the base than the most apical short-axis image. The cost function was optimized using the `fminunc` function in MATLAB (The Mathworks, Inc. Natick, MA), which uses a Quasi-Newton method with a mixed quadratic and cubic line search procedure. This cost function, however, is non-convex. When a long-axis slice is highly misregistered, the optimization algorithm could converge to a local minimum. Fig. 1 shows a plot of the cost function as a long-axis slice is shifted longitudinally from apex to base (solid line). The valleys in this plot are spaced one slice-thickness apart and occur when the apex in the long-axis contour gets close to one short-axis slice and then another. If a long-axis image is initially positioned in one of these valleys, the optimization algorithm may converge to the minimum of that valley instead of the global minimum of the cost function. To solve this problem, the first time this step was performed, the longitudinal contour distance was computed using a smoothed version of the true longitudinal contour distance (dashed line in Fig. 1). This step is denoted as "Smoothed LA registration" in Fig. 2.

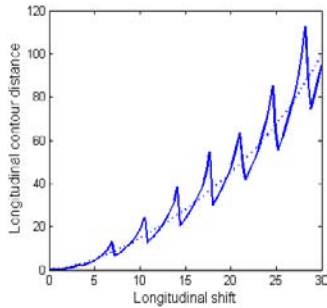


Fig. 1 Longitudinal contour distance cost function: actual (solid line) and smoothed (dashed line).

Third, each short-axis image was shifted in an in-plane direction to minimize the average distance between a short-axis contour and its counterpart in each long-axis image. These three steps were iterated until the final value of the cost function in step changes less than 0.01 mm between iterations as shown in Fig. 2. Note that two short-axis registration steps were used per iteration. The first short-axis registration can bring severely misregistered slices into alignment and can register short-axis slices that may be positioned below the most apical point in the long-axis contours. The second short-axis registration fine tunes the short-axis slice positions to match the long-axis contours.

To validate this algorithm contours were simulated from a prolate spheroidal model of the LV wall [2] (Fig. 3, right) with an epicardial diameter of 40mm at the base, a long-axis length of 76mm, and a wall thickness of 8mm. Registration errors were simulated by randomly shifting the slices in either an in-plane direction for short-axis slices or in 3D for long-axis slices. Each shift component was generated from a Gaussian distribution with standard deviations ( $\sigma$ ) ranging from 1 to 15mm. Ten trials were simulated for each value of standard deviation. The registration algorithm was then run on the misregistered data. Registration accuracy in the simulated contours was measured by the standard deviation of the centroids ( $Sd$ ) of both endocardial and epicardial contours in short-axis images and the mean distance ( $D$ ) of the centroids from the central LV axis in long-axis images. Note that both these quantities are zero in perfectly registered data. In the fifteen human studies, the registration accuracy was quantified by the average distance from the long-axis contours to the short-axis.

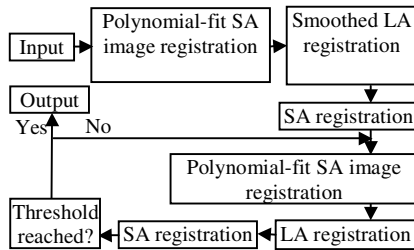


Fig. 2 Registration algorithm

## Results and Discussion

In the simulation experiments, the mean  $Sd$  and  $D$  values after registration are smaller than 0.001mm and 0.1 mm respectively for the entire range  $\sigma$  values (1-15mm). An example of severely misregistered slices ( $\sigma = 12$  mm) is shown in Fig. 3. The algorithm accurately registered the slices even though the initial registration was poor.

In human data, the average distance from long-axis to short axis contours was  $1.33 \pm 0.24$ mm, which was smaller than the pixel size in these images (1.50mm). Examples of registered end-diastolic contours are shown in Fig. 4.

## Conclusion

The simulation results demonstrate that the registration algorithm can register data sets with significant misregistration. Experimental results from human data demonstrate that the registration algorithm can adequately register short and long-axis images in human cardiac MR imaging studies.

## Acknowledgement

This work is supported by NIH NHLBI grant 1P50 HL77100-01.

## References

- [1] Cory Swingen et al., "An Approach to the Three-dimensional Display of Left Ventricular Function and Viability Using MRI," International Journal of Cardiovascular Imaging, Vol. 19, No. 4, pp. 325-336.
- [2] O'Dell, et al, Displacement field fitting for calculating 3D myocardial deformations from parallel-tagged MR images, Radiology, v 195, pp. 829-835, 1995.
- [3] Fully automated registration and warping of contrast-enhanced first-pass perfusion images. Journal of Cardiovascular Magnetic Resonance, Vol. 4, No. 4, pp. 459-69, 2002.

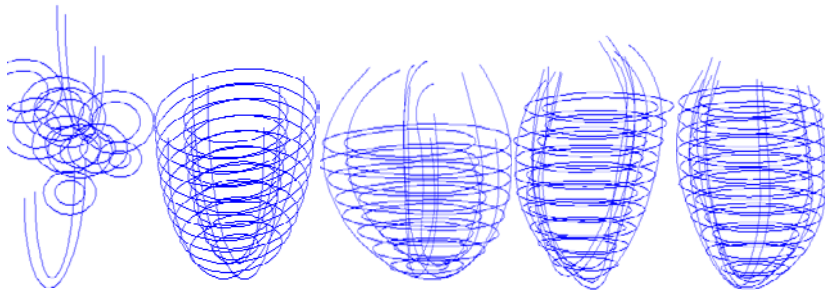


Fig. 3 Perturbed (left) and registered simulated contours

Fig. 4 Registered end-diastolic contours from three different human imaging studies.